Friction **6**(3): 316–322 (2018)
https://doi.org/10.1007/s40544-018-0239-1
ISSN 2223-7690
CN 10-1237/TH

RESEARCH ARTICLE

Single asperity friction in the wear regime

Yongjian YANG, Yunfeng SHI*

Department of Materials Science and Engineering, Rensselaer Polytechnic Institute, Troy, NY 12180, USA

Received: 02 May 2018 / Revised: 29 July 2018 / Accepted: 03 August 2018

Abstract: We used molecular dynamics simulation to investigate the friction of a single asperity against a rigid substrate, while generating debris. In the low wear regime (i.e., non-linear wear rate dependence on the contact stress, via atom-by-atom attrition), the frictional stress is linearly dependent on the normal stress, without any lubrication effect from the wear debris particles. Both the slope (friction coefficient) and friction at zero normal stress depend strongly on asperity-substrate adhesion. In the high wear regime (i.e., linear wear rate dependence on the contact stress, via plastic flow), the friction-normal stress curves deviate from a linear relation merging toward plastic flow of the single asperity which is independent of the interfacial adhesion. One can further link wear and friction by considering debris generation as chemical reaction, driven by both normal and frictional forces. The coupling between wear and friction can then be quantified by a thermodynamic efficiency of the debris generation. While the efficiency is less than 5% in the low wear regime, indicating poor mechanochemical coupling, it increases with normal stress toward 50% in the high wear regime.

Keywords: single-asperity contact; friction; molecular dynamics; atomic wear; plastic wear

1 Introduction

Friction and wear are two paramount questions in all tribological processes where two surfaces in relative motion are brought in contact. Examples of such contact range from conventional machineries (e.g., gears) [1] to tectonic boundary (e.g., earthquake) [2, 3] and to probe-based instrument for nanotechnology (e.g., atomic force microscopy (AFM)) [4, 5]. With a long history of human tribology practice dating back to at least ancient Egyptians [6], several empirical laws of friction, i.e., Amontons' laws [7–9], have been found and broadly applied: (1) the friction is proportional to the normal force, (2) the friction is independent of the apparent contact area, and (3) the kinetic friction is independent of the velocity. Recently, driven by device miniaturization and the complexity of multi-asperity contact, the focus of tribologists has been partially shifted to the single-asperity contact, well-defined between a slider-tip tribo pair [4,10–12]. Both experimental work and simulation work have provided new insights into the friction and wear mechanisms for single-asperity contact. For example, using molecular dynamics (MD), Mo et al. [8] have demonstrated that the friction force in a single-asperity contact is proportional to the contact area which is defined based on the number of atoms in contact. In our recent MD studies, we have demonstrated a transition from atomic wear to plastic wear in a single-asperity system and showed that the work of adhesion promotes such transition [13–15]. While the atomic wear is comprised of isolated debris and is generated at low load and low adhesion, the plastic wear involves collective debris formation from plastic flow at either high load or high interfacial adhesion. Both atomic wear and plastic wear have been quantified and the results are consistent with the experimental work by others [10, 12, 16]. The conditions for either mechanisms have been mapped out in the domain combining both the contact stress and the work of adhesion.

* Corresponding author: Yunfeng SHI, E-mail: shiy2@rpi.edu

As friction is often investigated in the wearless regime [17–21], appropriate for tribo-systems with negligible debris during sliding [13, 14, 18–20], it is interesting to examine the behavior of friction in the wear regime. Debris particles may affect the contact stress distribution as third bodies. At the same time, the debris generation is an additional energy dissipation mode which may affect friction. Specifically, we will leverage the single-asperity sliding system in our previous study on tip wear exhibiting atom-by-atom attrition to large debris cluster generation, in which the wear rate varies over four orders of magnitude [13, 16]. In this study, we focus on the frictional force (i.e., shear force) in the single-asperity contact system under different normal stress and interfacial adhesion. The effects of velocity, temperature and adhesion, and the mechanical work efficiency will be investigated. It appears that the friction is largely insensitive to the debris generation, following the same trend over wear rate spanning orders of magnitude. This is consistent with the weak chemo-mechanical coupling of the tribo-system, as quantified by the low thermodynamic efficiency of debris generation. Furthermore, friction force varies smoothly from atomic wear regime to plastic wear regime, with the thermodynamic efficiency of debris generation approaching 50%.

2 Simulation methodology

2.1 Simulation model

Two types of simulation setup have been used for the current study. One has been shown in Ref. [13], in which the system consists of an atomically-smooth rigid slider and a truncated-cone-shaped tip. The other setup is schematically shown in Fig. 1 in which a rectangular tip is used. The main advantages of using a rectangular tip include that (1) the contact area can be considered constant provided that the wear rate is small, so that the contact stress can be controlled by keeping the normal contact force at a constant value; and (2) smaller samples can be used for simulating over long period of time. Both the tip and the slider are made of glassy binary alloy interacting with the Wahnstrom potential [22]. The force field and the preparation of the samples are detailed in Ref. [13]. The slider is moving in the x-direction at a constant speed v varying from 0.01 to 30 m/s. The bottom of the tip is fixed by setting a rigid layer, above which a thermostat layer is set at a constant temperature T (*NVT* ensemble, Nose-Hoover thermostat) in order to maintain the temperature of the tip. For most sliding conditions used in this study, the interface temperature is close to the thermostat temperature. When the thermostat temperature is very low and the work of adhesion is high, the interface temperature can be 50 K higher than that of the thermostat temperature. The top part of the tip is simulated without pressure control or temperature control. For the rectangular tip, either periodic boundary conditions or non-periodic boundary conditions were used in the x-direction. The difference between these two types of condition is that the former does not allow tip atoms to leave the interface so that the height of the slider is not dropping, while the later allows tip atoms to leave the interface at the trailing end so that the height of the slider is continuously decreasing as a result of wear as seen in Refs. [13, 14]. We note that the friction is not sensitive to the boundary condition. In the z-direction (Fig. 1), periodic boundary conditions are used because we are interested in the friction and wear along the sliding direction (x-direction). We use LAMMPS package [23] to conduct all the MD simulations.

2.2 Tuning the work of adhesion

The work of adhesion between the tip and the slider is controlled by rescaling the bonding energy between the tip atoms and the slider atoms with a factor κ, i.e., $\varepsilon^{\text{Tip–Slider}} = \kappa\varepsilon$ where ε is the bonding energy of the tip or the slider [13]. As κ increases from 0.1 to 0.4, the work of the interface adhesion, W_{adh}, increases following a power law form [13] ($W_{\text{adh}} = a\kappa^b$ with a =

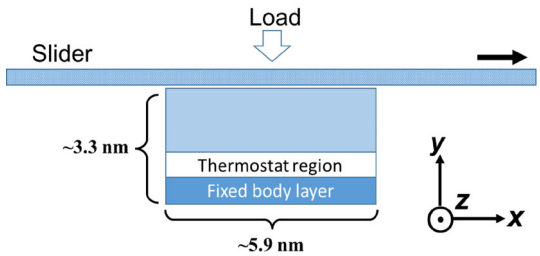

Fig. 1 Schematic of single asperity sliding model using a rectangular tip. The thickness of the sample in z-direction is about 5.0 nm.

1.29 J/m^2 and b = 1.5). Since there will be no interaction (attraction or repulsion) between the tip and the slider if κ is set to 0, to simulate a contact without adhesion, we use the original Lennard-Jones force field but set the potential cutoff at the bottom of the potential well (or $2^{1/6}\sigma$, in which σ is the Lennard-Jones length parameter). Note that when κ=0, there will still be friction due to the atomistic-level surface roughness between the slider and the tip.

2.3 Calculation of normal stress and shear stress

The normal contact stress and the shear stress are both calculated by dividing the normal force and frictional force with the nominal contact area. Because both stresses fluctuate with time, the average values and the standard deviation are reported where necessary. Under non-periodic boundary conditions in x-direction, debris atoms are generated and accumulate at the trailing end as shown in Fig. 2(a), where the change of the tip is relatively small and can be ignored for atomic wear. In the case of plastic wear, data from short sliding distance is used so that the change of tip shape can be safely ignored. In the current study, we define the wear debris as any tip atoms whose displacement is beyond a threshold value, following our previous study [13].

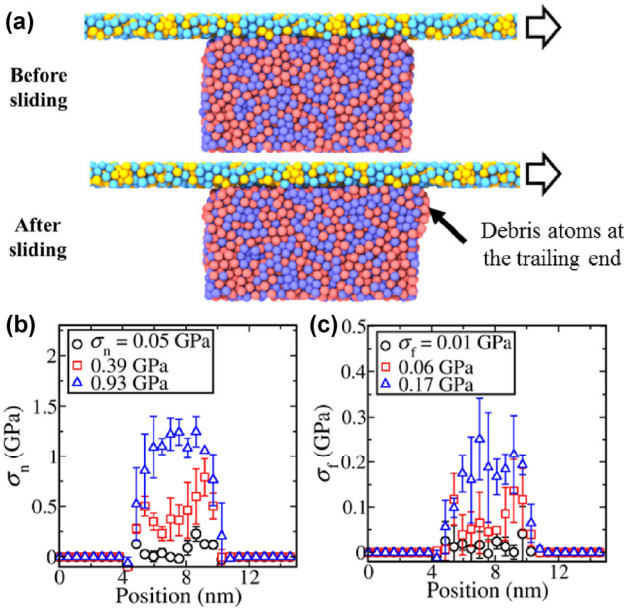

Fig. 2 (a) A side view of the sliding system before and after the sliding. As denoted by the arrow, some debris atoms (defined as atoms whose displacement is beyond a threshold value [13]) can be seen accumulating at the trailing end of the tip. Normal stress (b) and frictional stress (c) distribution along the sliding direction.

2.4 Calculation of the thermodynamic efficiency of debris generation

During the sliding, mechanical work done by sliding/compression is dissipated via both atomic/plastic wear and frictional heat. One can consider debris generation as chemical reaction, driven by mechanical work. Therefore, the conversion of mechanical energy to chemical energy (stored in the debris particles) can be quantified by a thermodynamic efficiency, characterizing the strength of mechanochemical coupling between the friction and wear. As the energy associated with wear is correlated with the potential energy change of the slider-tip system during sliding, the thermodynamic efficiency can be computed from the ratio of the potential energy change over the mechanical work done (including work done by shear force in the sliding direction and work done by normal force in the loading direction).

3 Results and discussion

3.1 Normal/friction stress distribution along the sliding direction x

At the beginning of the sliding, the frictional force increases monotonically due to the elastic deformation of the tip until it reaches a peak value as seen in both experiments and simulations by Refs. [17, 24]. Thereafter, the system reaches a steady state where the frictional force fluctuates around an average value. The steady state can be easily achieved in the binary Lennard-Jones tribo-system as demonstrated in our previous study [13]. Figures 2(b) and 2(c) show the distribution of normal stress and shear stress along the sliding direction. Finite element modeling on similar geometry has shown a singularity of normal stress at the leading edge between a post and rigid surface [25]. However, no stress singularity is observed because of the breakdown of continuum elasticity for our discrete MD model. Along the sliding direction, the values of both normal stress and shear stress are relatively constant.

3.2 Temperature dependence of the frictional stress

The influence of temperature and velocity on the frictional stress is shown in Fig. 3. We found in most cases the change of the frictional stress with temperature is generally minor. For low adhesion, such as W_{adh} = 0.04 J/m^2, there seems to be a small increase of frictional stress with the temperature when the normal stress is smaller than 0.6 GPa. Beyond that, the frictional stress change with temperature can be ignored considering its statistical variation.

For high adhesion, such as W_{adh} = 0.16 J/m^2, the situation is different in that the frictional stress is unchanged for normal stress up to 0.4 GPa, and then decreases with the temperature at higher normal stress. For example, the frictional stress for the normal stress of 1.2 GPa decrease from 0.51 GPa at T = 63 K to 0.42 GPa at T = 535 K. The drop of frictional stress with temperature at high work of adhesion has been observed by Spijker et al. [26] and is probably due to the softening of the tip material under high shear stress (the glass transition temperature of the tip has been estimated to be ~1,000 K [13]). The influence of the temperature on the dependence of the shear stress on the normal stress can be ignored in low adhesion case as shown in Fig. 3(c) whereas at high adhesion and high temperature, the slope, i.e., friction coefficient could drop at relatively high temperatures, as seen in Fig. 3(d).

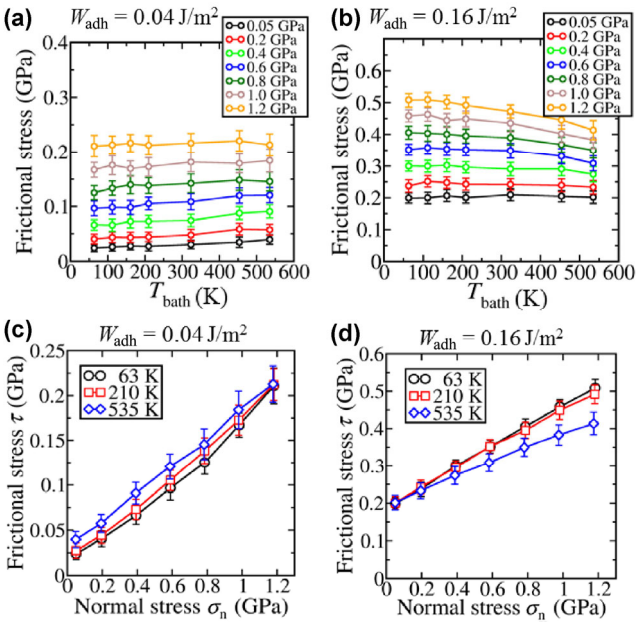

Fig. 3 (a, b) Variation of shear stress with the bath temperature at two levels of work of adhesion using periodic boundary conditions. The normal stress during sliding is shown in the legend. (c, d) Frictional stress as a function of normal stress at two levels of work of adhesion at different temperatures.

3.3 Velocity dependence of the frictional stress

The dependence of the frictional stress on the velocity is shown in Fig. 4, where the shear stress is independent of the sliding speed spanning almost four orders of magnitude. Because the velocity in our simulation is much larger than the typical scanning speed used in AFM (<10^{-5} m/s), it may be possible that the friction decreases at much lower sliding velocity as seen in the experiments predicted from a thermal activation friction model [27]. On the other hand, when the sliding speed is increased to more than 30 m/s, there is a small amount of increase in friction, possibly due to the viscous damping for which the frictional force is proportional to the sliding velocity [28]. We also note that the velocity independence of the friction has also been observed by Zwörner et al. [28] in the range of nm/s to μm/s between a silicon tip and carbon compounds when the sliding velocity is smaller than the velocity of tip slip.

3.4 Relation between the frictional stress and the normal stress

With increasing normal stress, the single asperity sliding experiences a transition from the atomic wear mechanism to the plastic wear mechanism as seen in

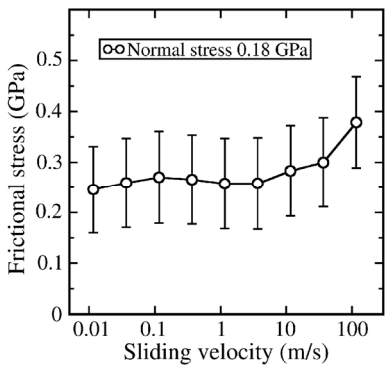

Fig. 4 Variation of shear stress with sliding velocity at the normal stress of 0.18 GPa. W_{adh} = 0.16 J/m^2 and T = 63 K. The sliding velocity is varied from 0.01 to 116 m/s.

Ref. [13]. Due to geometrical limitation, the simulation setup (Fig. 1) does not allow the plastic wear to occur via shear deformation in an angle declining along the sliding direction if the slip line touches the bottom of the tip. Therefore, sliding simulation using a truncated cone tip is more appropriate in this case [10]. The frictional stress as a function of normal stress is shown in Fig. 5(a). It can be found in the atomic wear region and under different work of adhesions that, the frictional stress increases linearly with the normal stress, which can be well fitted with a linear function: $\tau = \tau_0 + \mu\sigma_n$. Both τ_0 and μ depend sensitively on interfacial adhesion. From the linear fitting in Fig. 5(a), τ_0 and μ are plotted against the adhesion factor κ in Fig. 5(b). In the plastic wear region, the frictional stress-normal stress curves start to deviate and merge into a master curve, see the white dash line in Fig. 5(a) (a yield surface that can be described by Mohr-Coulomb yield criterion [29, 30]), which corresponds to plastic yielding of the single-asperity, independent of interfacial adhesion.

It is important to note that, in the atomic wear region, there are atomic wear debris constantly generated at the interface. Intuitively, one may expect that the atomic wear particles could serve to lubricate the interface and therefore reduce the friction [31]. However, as shown in Fig. 5(a), the friction coefficient stays constant for the entire range of normal stress, spanning wear rate (see Ref. [13]) over three orders of magnitude. It appears that debris particles generated at the tribo-interface, without chemical alteration such as oxidation, may not be considered as third bodies.

3.5 Efficiency of the mechanical work

The efficiency for sliding simulation with a truncated cone at different work of adhesion is shown in Fig. 6. There exists a transition of the thermodynamic efficiency of debris generation from low normal stress (atomic wear) to high normal stress (plastic wear) which is in correspondence with the wear rate transition between the atomic wear regime and the plastic wear regime [13]. In the low wear regime, less than 5% mechanical energy is dissipated through wear and most of the mechanical energy is converted to frictional heat. Debris generation can be considered as chemical reaction, driven by the mechanical agitation of the slider [12]. Thus, the low mechanical efficiency in the low wear regime indicates a poor mechanochemical coupling between friction and wear. For high normal stress, the thermodynamic efficiency increases with the normal stress, in a manner similar to the wear rate in the plastic wear region [13]. It can be also seen in Fig. 6 that, at very high normal stress, all three curves saturate to an efficiency of roughly 50%, where the normal stress is very close to the tip crushing stress ~2.5 GPa [13]. That is, the mechanical work is equally dissipated by wear, i.e., plastic flow, and frictional heat, which is somewhat similar to the equipartition of kinetic energy and potential energy in a harmonic oscillator in equilibrium. Recently, Aghababaei et al. [32] have discovered a linear dependence of the wear debris volume on the frictional work in single-asperity wear via fracture-induced debris, which is a clear evidence that part of the

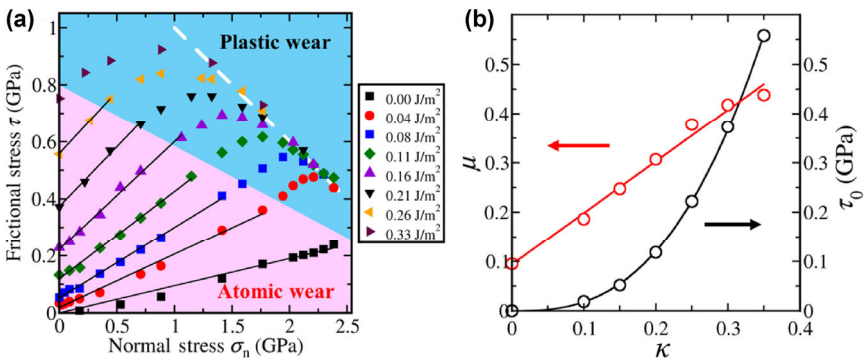

Fig. 5 (a) Frictional stress as a function of normal stress and work of adhesion. The boundary between atomic wear (purple region) and plastic wear (blue region) is schematically drawn according to Ref. [13]. The largest normal stress, ca. 2.52 GPa corresponds to tip crash stress and the largest shear stress, ca. 1.05 GPa corresponds to κ = 100%. The yield surface is denoted by the white dash line in the plastic wear regime. (b) τ_0 and μ from linear fitting in (a) at different κ (the linear fitting for W_{adh} = 0.00 J/m^2 is forced to pass the origin).

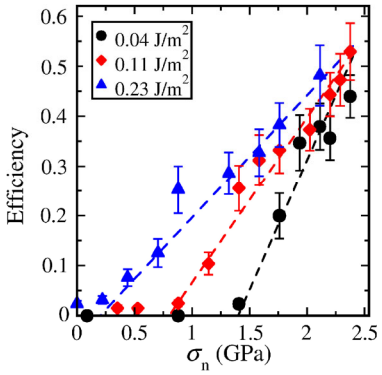

Fig. 6 Variation of the efficiency of the mechanical work with normal stress at three levels of adhesion. The dash lines are guides for eyes to show the linear dependence of the efficiency on normal stress in the plastic wear regime.

mechanical work is spent on wear debris generation. Since the authors have not reported any data on the frictional heat during the sliding, it will be very interesting to measure the efficiency of the mechanical work in this type of wear.

4 Conclusions

For single-asperity sliding system, we have found the friction is generally independent of temperature or sliding velocity within our simulation range. In the atomic wear region, Amontons' first law is observed from the linear dependence of the frictional stress on the normal stress. No lubrication effect from wear debris particles is observed. The frictional stress deviates from the linear trend in the plastic wear regime until the tip crashes. The low efficiency (<5%) of the mechanical work in the atomic wear regime indicates a poor coupling between wear and friction. In the plastic wear regime, the mechanical efficiency increases linearly with normal stress toward 50%.

Acknowledgement

We thank Professors Liping Huang (Rensselaer Polytechnic Institute), Thierry Blanchet (Rensselaer Polytechnic Institute), Izabela Szlufarska (Univ. of Wisconsin), Rob Carpick (Univ. Pennsylvania), Mark Robbins (Johns Hopkins) and Michael Falk (Johns Hopkins) for useful discussions. We are grateful to the support from the National Science Foundation (Grant No. CMMI-1031408). Molecular dynamics simulations were carried out in LAMMPS using supercomputers in the Computational Center for Innovations (CCI) at RPI.

References

[1] Bowden F P, Tabor D. *The Friction and Lubrication of Solids*. Oxford (UK): Oxford University Press, 2001.

[2] Scholz C H. Earthquakes and friction laws. *Nature* **391**(6662): 37–42 (1998)

[3] Brace W F, Byerlee J D. Stick-slip as a mechanism for earthquakes. *Science* **153**(3739): 990–992 (1966)

[4] Szlufarska I, Chandross M, Carpick R W. Recent advances in single-asperity nanotribology. *J Phys D Appl Phys* **41**(12): 123001 (2008)

[5] Carpick R W, Salmeron M. Scratching the surface: Fundamental investigations of tribology with atomic force microscopy. *Chem Rev* **97**(4): 1163–1194 (1997)

[6] Dowson D. *History of Tribology*. London (UK): Longman Group Limited, 1979.

[7] Gao J P, Luedtke W D, Gourdon D, Ruths M, Israelachvili J N, Landman U. Frictional forces and amontons' law: From the molecular to the macroscopic scale. *J Phys Chem B* **108**(11): 3410–3425 (2004)

[8] Mo Y F, Turner K T, Szlufarska I. Friction laws at the nanoscale. *Nature* **457**(7233): 1116–1119 (2009)

[9] Archard J F. Elastic deformation and the laws of friction. *Proc Roy Soc A* **243**(1233): 190–205 (1957)

[10] Gotsmann B, Lantz M A. Atomistic wear in a single asperity sliding contact. *Phys Rev Lett* **101**(12): 125501 (2008)

[11] Jacobs T D B, Gotsmann B, Lantz M A, Carpick R W. On the application of transition state theory to atomic-scale wear. *Tribol Lett* **39**(3): 257–271 (2010)

[12] Jacobs T D B, Carpick R W. Nanoscale Wear as a stress-assisted chemical reaction. *Nat Nanotechnol* **8**(2): 108–112 (2013)

[13] Yang Y J, Huang L P, Shi Y F. Adhesion suppresses atomic Wear in single-asperity sliding. *Wear* **352–353**: 31–41 (2016)

[14] Vargonen M, Yang Y J, Huang L P, Shi Y F. Molecular simulation of tip Wear in a single asperity sliding contact. *Wear* **307**(1–2): 150–154 (2013)
[15] Yang Y. Quantitative understanding of single-asperity contact via molecular simulations. Ph.D Thesis. Rensselaer Polytechnic Institute, 2017.
[16] Sha Z D, Sorkin V, Branicio P S, Pei Q X, Zhang Y W, Srolovitz D J. Large-scale molecular dynamics simulations of wear in diamond-like carbon at the nanoscale. *Appl Phys Lett* **103**(7): 073118 (2013)
[17] Li Q Y, Dong Y L, Perez D, Martini A, Carpick R W. Speed dependence of atomic stick-slip friction in optimally matched experiments and molecular dynamics simulations. *Phys Rev Lett* **106**(12): 126101 (2011)
[18] Gnecco E, Bennewitz R, Gyalog T, Loppacher C, Bammerlin M, Meyer E, Güntherodt H J. Velocity dependence of atomic friction. *Phys Rev Lett* **84**(6): 1172–1175 (2000)
[19] Riedo E, Gnecco E, Bennewitz R, Meyer E, Brune H. Interaction potential and hopping dynamics governing sliding friction. *Phys Rev Lett* **91**(8): 084502 (2003)
[20] Sang Y, Dubé M, Grant M. Thermal effects on atomic friction. *Phys Rev Lett* **87**(17): 174301 (2001)
[21] Jansen L, Hölscher H, Fuchs H, Schirmeisen A. Temperature dependence of atomic-scale stick-slip friction. *Phys Rev Lett* **104**(25): 256101 (2010)
[22] Wahnström G. Molecular-dynamics study of a supercooled two-component Lennard-Jones system. *Phys Rev A* **44**(6): 3752–3764 (1991)
[23] Plimpton S. Fast parallel algorithms for short-range molecular dynamics. *J Comput Phys* **117**(1): 1–19 (1995)
[24] Luan B Q, Robbins M O. Effect of inertia and elasticity on stick-slip motion. *Phys Rev Lett* **93**(3): 036105 (2004)
[25] Minsky H K, Turner K T. Achieving enhanced and tunable adhesion via composite posts. *Appl Phys Lett* **106**(20): 201604 (2015)
[26] Spijker P, Anciaux G, Molinari J F. Relations between roughness, temperature and dry sliding friction at the atomic scale. *Tribol Int* **59**: 222–229 (2013)
[27] Liu X Z, Ye Z J, Dong Y L, Egberts P, Carpick R W, Martini A. Dynamics of atomic stick-slip friction examined with atomic force microscopy and atomistic simulations at overlapping speeds. *Phys Rev Lett* **114**(14): 146102 (2015)
[28] Zwörner O, Hölscher H, Schwarz U D, Wiesendanger R. The velocity dependence of frictional forces in point-contact friction. *Appl Phys A* **66**(S1): S263–S267 (1998)
[29] Vargonen M, Huang L P, Shi Y F. Evaluating Mohr–Coulomb yield criterion for plastic flow in model metallic glasses. *J Non Cryst Solids* **358**(24): 3488–3494 (2012)
[30] Lund A C, Schuh C A. Yield surface of a simulated metallic glass. *Acta Mater* **51**(18): 5399–5411 (2003)
[31] Berman D, Deshmukh S A, Sankaranarayanan S K R S, Erdemir A, Sumant A V. Macroscale superlubricity enabled by graphene nanoscroll formation. *Science* **348**(6239): 1118–1122 (2015)
[32] Aghababaei R, Warner D H, Molinari J F. On the debris-level origins of adhesive wear. *Proc Natl Acad Sci USA* **114**(30): 7935–7940 (2017)

Yunfeng SHI. He received his Ph.D. degree in materials science from the University of Michigan, Ann Arbor, in 2006. He then spent two years in North Carolina State University as a postdoctoral research associate. Dr. Shi joins the Department of Materials Science and Engineering at Rensselaer Polytechnic Institute in Fall 2008 as an assistant professor and was promoted to associate professor in 2014. His research focuses on simulation and modeling of advanced materials systems. His recent interests include nanoporous carbon, molecular motors, energetic materials, nano-tribology and metallic glasses.

Yongjian YANG. He received his Ph.D. degree in materials engineering from Rensselaer Polytechnic Institute in Troy, New York in 2017. Now he is a postdoctoral scholar at the Penn State University in State College. His research interests include nano-tribology, glass science, metal-organic framework, etc., using molecular simulation.